Available online at www.sciencedirect.com
ScienceDirect
Journal of the European Ceramic Society 29 (2009) 355–362
www.elsevier.com/locate/jeurceramsoc

High temperature creep and tensile properties of alumina formed on Fecralloy foils doped with yttrium

S.K. Sharma, G.D. Ko, K.J. Kang *

Department of Mechanical Engineering, Chonnam National University, Gwangju 500-757, Republic of Korea

Received 2 June 2007; received in revised form 21 May 2008; accepted 30 May 2008
Available online 30 July 2008

Abstract

The three batches of Fecralloy foils, which differ from each other in contents of yttrium, that is, 10, 280 and 560 ppm, respectively, were chosen as the thermally grown oxide (TGO), alumina (α-Al_2O_3) forming substrate. The creep tests were performed with the Fecralloy foils, which have the α-Al_2O_3 TGO of 0–4 μm thickness, on the surfaces. The creep rates decreased as the TGO thickness increased. The yttrium content above 280 ppm delayed the creep rate of the Fecralloy substrate. The higher creep rate than that of the stand-alone polycrystalline alumina and the dependency of the creep rate on TGO thickness agrees with the hypothesis that the high temperature creep of the TGO is a consequence of the inter-grain growth of the TGO. The yttrium content of lower than 560 ppm did not affect on the creep rate of TGO. Tensile tests were performed with the same alloys, which have the α-Al_2O_3 TGO of 0–3 μm thickness. The tensile strength of the substrate itself increased with Y content by ∼20%. The tensile stress of the α-Al_2O_3 TGO decreased with Y-content but it is almost constant, regardless of the TGO thickness. The peak stresses were found at the strain range of $\varepsilon = 0.7$–1.5%, regardless of the TGO thickness, and the batches, thereafter, the parallel cracks perpendicular to the loading direction, formed on the surface. The obtained stress–strain curves of TGO fluctuated. It showed a common feature, that is, a sharp stress drop after the initial yield point at $\sigma_Y = 40$–85 MPa, but the stress increased again until the peak points, $\sigma_{UTS} = 50$–110 MPa.

Keywords: Fecralloy; Thermally grown oxide; Alumina; Creep and tensile properties

1. Introduction

Thermally grown alumina (α-Al_2O_3) forms on aluminum containing alloys, for example NiAl, FeCrAl, at high temperature in air due to the mechanism of outward diffusion of metal cation and inward diffusion of oxygen anions.[1–9] Alumina exhibits better anticorrosion properties than other oxides such as Cr_2O_3, FeO, at high temperature because of its slowly growing, dense microstructure and good adherence. A major concern in the oxidation behavior of alumina-forming alloys and coatings is the ability of the oxide scale to withstand repeated thermal fatigues in high temperature applications, such as gas turbine blades, vanes, combustors and so on.[6,10–14] Therefore, it is necessary to understand the growth mechanisms and mechanical strengths of oxides.

The mechanism of α-Al_2O_3 oxide growth on FeCrAl has been investigated. Equiaxed α-Al_2O_3 scales were found to grow by diffusion of simultaneous outward Al cations and inward oxygen anions diffusion on undoped FeCrAl, whereas a columnar α-Al_2O_3 grain structures were produced on Y-doped FeCrAl by inward oxygen diffusion as outward Al diffusion was suppressed.[15–18] Also yttrium tends to promote α-Al_2O_3 with finer grains.[19] The dimensions of the columnar grains were approximately 1–2 μm in length and 0.4–0.6 μm in width.[15] Microstructural studies have shown that the addition of yttrium to an alumina forming alloy commonly results in an α-Al_2O_3 scale, which tends to be very flat in the absence of voids at the interface. This improvement is caused by Y_2O_3 particles that key the substrate to the oxide scale,[20] whereas the yttrium-free alloys tend to form a convoluted scale with interface voids.[21] In addition, one more significant effect of yttrium, that is, the reduction in growth rate of the oxide scale, is due to reduced cation diffusivity.[22] Amano et al. found that the Y-content gives good adherence on FeCrAl. The oxide scale could not be spalled from the substrate.[23]

* Corresponding author. Tel.: +82 62 530 1668; fax: +82 62 530 1689.
E-mail address: kjkang@chonnam.ac.kr (K.J. Kang).

0955-2219/$ – see front matter © 2008 Elsevier Ltd. All rights reserved.
doi:10.1016/j.jeurceramsoc.2008.05.051

Table 1
Chemical composition of Fecralloy foils

	Fe (%)	Cr (%)	Al (%)	Mn (ppm)	Si (ppm)	Zr (ppm)	Ti (ppm)	Y (ppm)
Batch-I	73.6	21.4	4.71	790	310	1300	160	10
Batch-II	72.9	21.7	5.30	1560	560	720	800	280
Batch-III	73.3	21.4	5.10	1450	440	800	510	560

The mechanical properties of thermally grown α-Al_2O_3 thin films are important for the assessment and maintenance of the protective effect of the films under operating conditions. The properties of a material in the shape of the thin film are often different from those of a bulk because of the scale effect and anisotropic microstructure. Also, there might be metallurgical interaction between the TGO and the substrate. The mechanical properties of bulk α-Al_2O_3 for high temperature ceramic structural applications have been studied in detail.[24–32] French et al. reported that the tensile creep rate of bulk α-Al_2O_3 decreased by ∼2 orders of magnitude by the addition of 1000 ppm Y, that is, Y-doped alumina strain hardened, and as a result, the strain rate decreased with increasing strain.[30] They attributed this effect to the strong segregation of Y to the alumina grain boundaries. In continuation to Cho et al. and French et al. investigated the creep rates of bulk polycrystalline alumina doped with rare earth elements such as Y and La.[28,30] They found lower creep rate in doped α-Al_2O_3 than in pure α-Al_2O_3.

Schutze and his colleagues used a 4-point bend test to measure the mechanical properties of TGOs formed on metal substrates, i.e., Ni, TiAl and mild steels.[33–35] This technique was suitable only for TGO thickness of more than 100 μm and failed for TGO thickness of less than 100 μm due to spallation and cracks. Except for this, data on the mechanical properties of TGO formed on metal substrates were hardly found in the literature.

Recently, Kang and Mercer reported a new method for *in situ* measurement of creep behavior of α-Al_2O_3 TGO of 1–4 μm in thickness, formed on Fecralloy doped with yttrium contents of 280 and 560 ppm at high temperature.[36] The steady state creep rates were found to be higher than that of the bulk polycrystalline α-Al_2O_3. These rates considerably decreased as the α-Al_2O_3 TGO thickness increased. The yttrium contents also influenced the creep rate by forming Y_2O_3 or YAG, as in the bulk polycrystalline α-Al_2O_3. The changes in the specimen length under negligible applied stress also suggested that the amount of yttrium could have influenced the growth strain as well as the creep rate.

In continuance with the earlier work, the objective of this work is to study not only the creep properties of α-Al_2O_3 TGO formed on the lower Y doped alloy, but also the tensile properties. Namely, three batches of alloy foils, including a batch with virtually no yttrium content, were used. Creep tests were performed for the lowest Y-doped batch having α-Al_2O_3 TGO of 1–4 μm thickness on the surfaces. And tensile tests were performed on the three batches with α-Al_2O_3 TGO of 0–3 μm thickness on the surfaces.

2. Experimental protocol

2.1. Materials and preparation

The creep and tensile tests were performed on an alumina forming, commercially available heat resistant alloy, Fecralloy. Three batches of Fecralloy were acquired in the form of cold-rolled foils having a thickness of 100 μm. The chemical compositions were analyzed by the Atomic Emission Spectrometer (PerkinElmer, OPTIMA 4300 DV). The results are listed in Table 1. They differ primarily in Y: with batch-I containing 10 ppm; batch-II containing 280 ppm and batch-III containing 560 ppm. These foils were cut into ribbons with lateral dimensions of ∼5 mm × 50 mm. Thereafter, they were annealed and polished. The detailed process is given in the previous work.[36]

2.2. Test systems

For the measurement of creep properties of alumina TGO, a novel micro-creep test system has been used, that is the same as well as in the earlier work.[36] For tensile tests, the specimens were loaded by a specially designed micro-tensile test machine. Micro-tensile test machine is shown in Fig. 1. Its specifications are given in Table 2. The loading actuator was a stepping motor and it was capable of controlling the conveying distance with a resolution of 0.05 μm. A CCD camera with a zoom lens was placed in front of the test rig to obtain a series of digital images on the specimen gage. In order to keep the heat generated by the specimen from being transferred to the load cell, a compact water cooler was installed between the upper grip and the load cell.

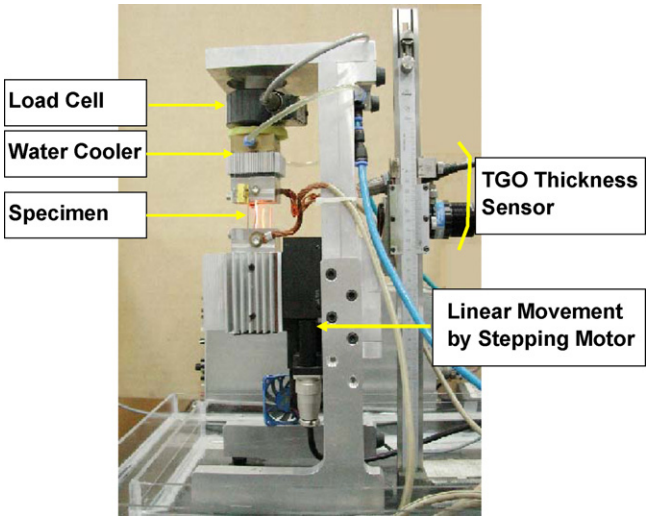

Fig. 1. Micro-tensile test system with TGO thickness sensor (right).

Table 2
Specifications of the micro-tensile tester

Properties	Range	Precision
Load	0–20 N	0.02 N
Displacement	−10 ∼ +10 mm	0.05 μm
TGO thickness	0–5 μm	0.1 μm
Temperature	*RT* ∼ 1300 °C	3 °C
Specimen size	ength: 40–100 mm, thickness: 0.05–1 mm, width: 4–10 mm	
Temperature slew rate	50 °C/s	
Minimum period of load cycle	200 s in the full range of displacement	

Two IR pyrometers, each having different wavelengths, were installed in the rear of the test rig in order to measure the TGO thickness by EDM and temperature *in situ*.[37]

2.3. Test and measurement procedure

To determine the creep or tensile properties of the substrate, itself, the Fecralloy specimens were heated to 1200 °C in pure dry argon environment, and load was applied and the displacements were measured. The TGO formed during these tests was determined to be minimal (thickness < 0.3 μm). When the specimens were heated to such a high temperature, they radiated like a filament of a light bulb.

To measure the creep properties of the TGO, the same procedure as in the earlier work[36] was adopted. Before the tensile tests, the alumina powder (particle size: 0.05 μm)–water mixture was sprayed on each specimen gage-section and dried for 2 h at 100 °C in an electric oven. This left clear random dots on the surface, as shown in Fig. 2. The dots on the surface of the tensile specimen enabled strain mapping of the images taken during the test. Namely, the dots served as the speckle pattern, which was used to measure the displacement via the Digital Image Correlation (DIC) technique. Fig. 3 shows the examples of the images of a specimen surface taken by the CCD camera. In the images, the two inserts show contours of displacement distribution measured via DIC software, VIC-2D

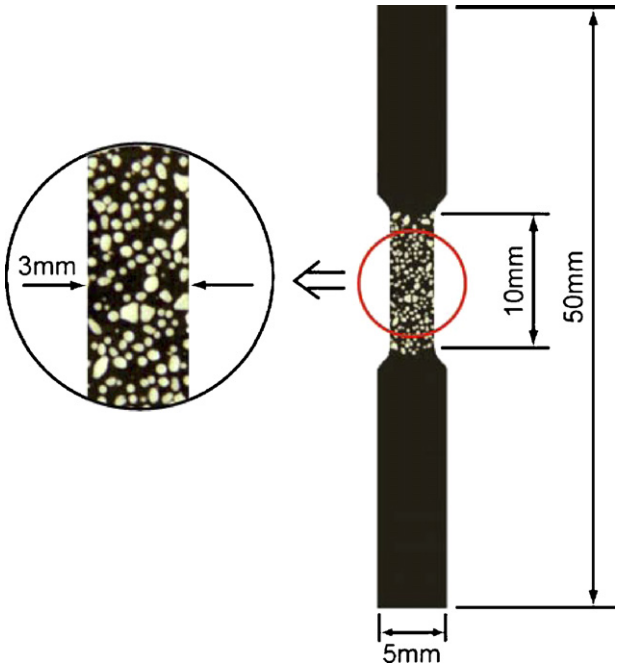

Fig. 2. Configurations of micro-tensile specimens and random dots sprayed on a specimen's gage section.

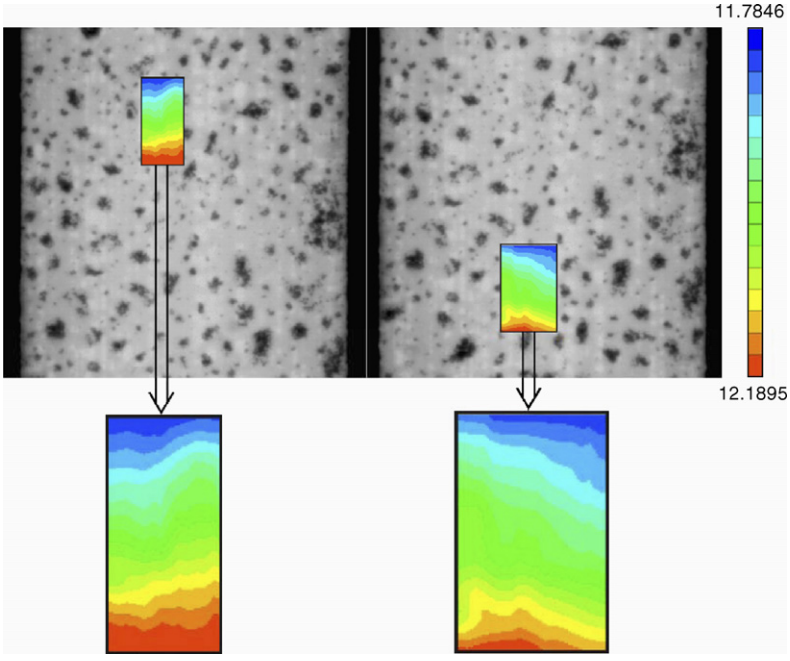

Fig. 3. Images taken from the specimen surface during a tension test at 1200 °C and the inserts are contour maps of displacement in the vertical direction around two points on the specimen (left: upper point; right: lower point).

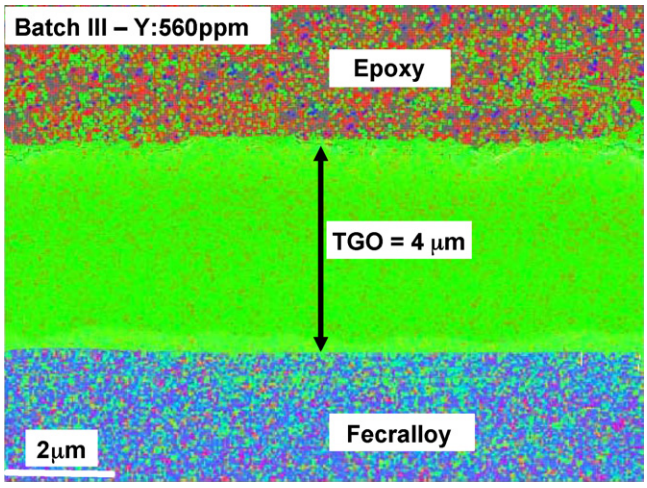

Fig. 4. SEM mapping of cross section around TGO formed on the highest Y-containing substrate (batch-III).

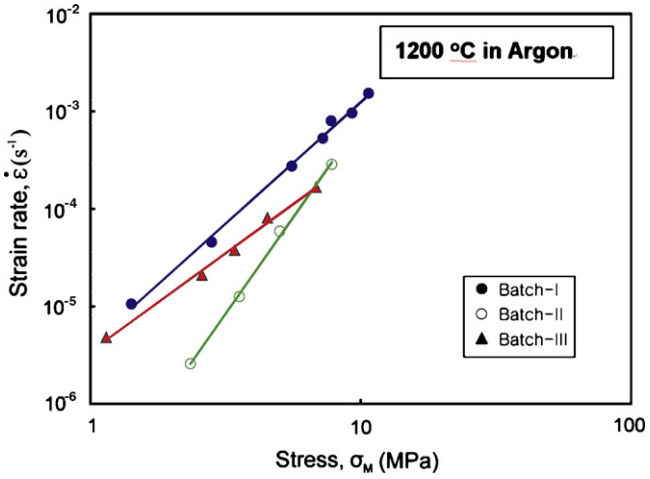

Fig. 5. Creep strain rate versus applied stress of Fecralloy itself of three different contents of Y: 10, 280 and 560 ppm measured in Argon ambient at 1200 °C.

(http://www.correlatedsolutions.com). During the tensile test, the displacement was controlled at a speed of 10 μm/s.

2.4. Characterization

The weight and dimensions were measured before and after each test. The polished cross sections were used to check the TGO thickness. The scanning electron microscope (SEM) mapping and energy-dispersive spectroscopy (EDS) were employed to obtain compositional information of the TGO and the alloy. A SEM-mapping for the TGO with the highest yttrium content, i.e., the batch-III, is shown in Fig. 4. The elements presented in α-Al_2O_3 TGO and Fecralloy itself were also confirmed by EDX measurements. The TGO exhibited dense, uniform, void free interface (TGO/alloy) and only α-Al_2O_3 matrix.

3. Result and discussion

3.1. Creep properties

The creep responses of the Fecralloy substrate itself of three different yttrium contents, respectively, are shown in Fig. 5. These preliminary test results can be fitted to a formula of steady state creep: $\dot{\varepsilon}_{ss}/\dot{\varepsilon}_0 = (\sigma/\sigma_0)^n$, with a reference strain-rate, $\dot{\varepsilon}_0$ (taken to be $\dot{\varepsilon}_0 = 10^{-6}\ s^{-1}$). In this formula, the reference stress, $\sigma_0 = 0.58$ MPa, $n = 2.5$ for the batch-I alloy; $\sigma_0 = 1.85$ MPa, $n = 4$ for the batch-II alloy, and $\sigma_0 = 0.55$ MPa, $n = 2$ for the batch-III alloy were obtained. These relations were to be used to deconvolute the stress supported by the substrate in the following measurements, upon consideration that the strain-rate must be identical in the substrate and TGO. Fig. 5 shows that at a given strain rate, the stress associated with yttrium concentration of 280 ppm was higher than that with concentrations of 10 and 560 ppm. When the strain rate was around $\dot{\varepsilon} \approx 10 \times 10^{-6}\ s^{-1}$, the stress level was about 1–3 MPa.

When the TGO formed on specimen's surface, however, regardless of the Y content, the substrate had virtually no contribution on the creep resistance, as shown in the previous work[36] for the batch-III alloy. Namely, when stress acting in TGO was calculated by $\sigma_{TGO} = P/2Wh$ based on the assumption that the TGO sustained all the external forces, as illustrated in Fig. 6, the test results with different thicknesses of the substrate, H, in atmosphere revealed no difference in $\dot{\varepsilon}$–σ_{TGO} curves for a given TGO thickness, h, provided that TGO thickness, h, and the substrate thickness, H, were in a range of $h > 1$ μm and $H < 400$ μm. The steady-state creep results of α-Al_2O_3 TGO of thicknesses from 1 to 4 μm of all the three batches obtained below 200 MPa are summarized in Fig. 7. For batches I and II, the steady state creep behaviors coincided with each other

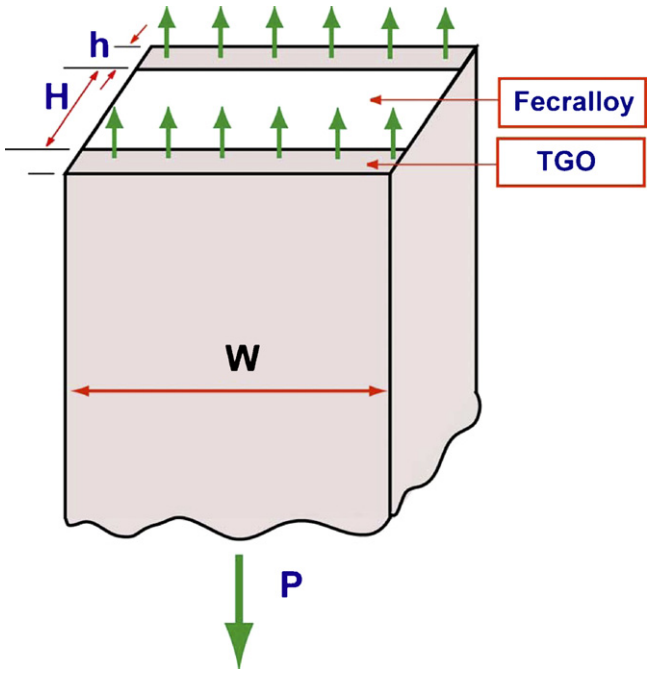

Fig. 6. Illustraion of stress distribution in TGO under the external load, P, when the substrate has no strength.

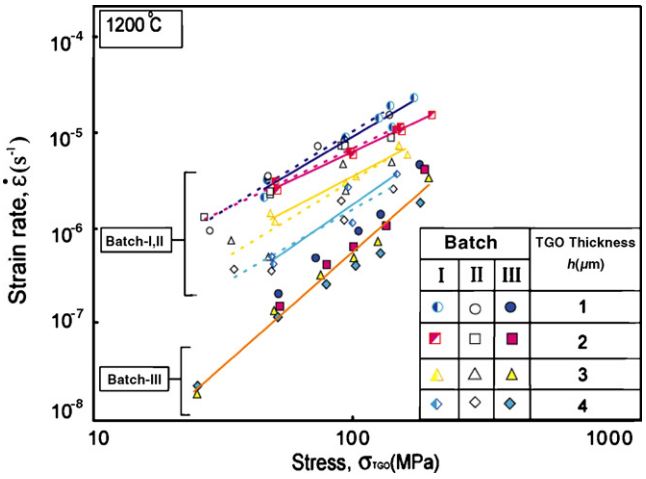

Fig. 7. Strain rate versus stress-in-TGO data measured from creep tests of batches I, II and III with TGO of four different thicknesses: $h = 1$, 2, 3 and 4 μm.

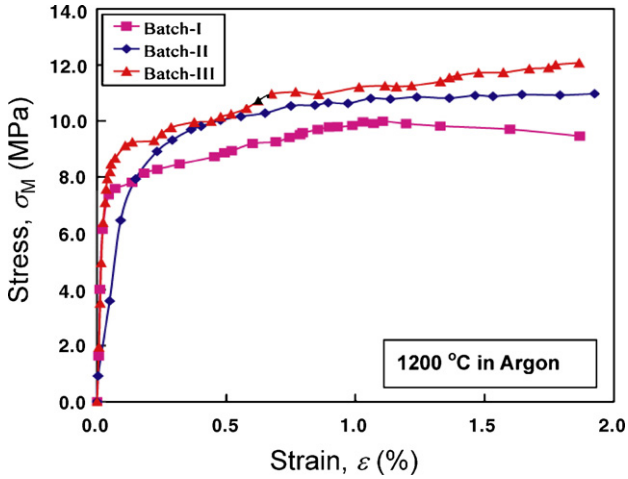

Fig. 9. Stress–strain curves of Fecralloy substrates of batches I, II and III obtained from tension tests at 1200 °C in Argon ambient.

with in an experimental error range. TGO thickness significantly affected the creep rate, that is, the creep rate decreased with TGO thickness. On the other hand, for batch-III which contained the highest Y, creep behaviors were totally different from the other two batches. The creep rates were much lower and the dependency on TGO thickness was substantially weakened. However, even for batch-III, when the creep rates are plotted against TGO thickness as shown in Fig. 8, the dependency on TGO thickness is obvious. This agrees with the hypothesis of the author's previous work.[36] Namely, the deformation of the TGO under tensile stress at high temperature is not a result of typical creep mechanisms such as diffusion of vacancies or intragranular motion of dislocations,[38–39] but a result of intergrain growth of TGO, that is, generation of new oxide along the grain boundaries perpendicular to the loading direction causes the lengthening. Therefore, a thicker TGO means a longer path for the ions, which results in the lower rate of deformation as a kind of creep.

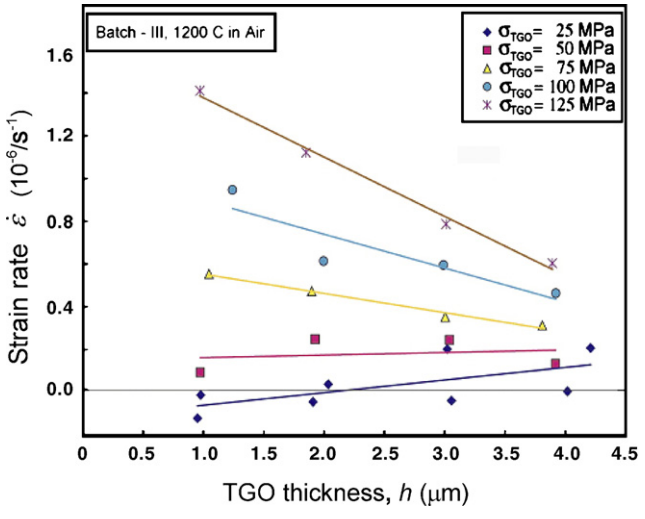

Fig. 8. The creep rates, $\dot{\varepsilon}_{ss}$, versus TGO thickness, h, under various applied stresses measured from the batch-III specimens.

3.2. Tensile properties

Fig. 9 shows the tensile stress–strain curves for the substrate itself of the three batches tested in the argon environment. The curve shows that the yield strength, σ_Y, increases from 7.6 to 9.2 MPa as the yttrium content increases from batch-I (Y: 10 ppm) to batch-III (Y: 560 ppm). At strain ~1%, the stress increases from 9.8 to 11.2 MPa with the increase of yttrium content.

The total load versus strain curves for specimens oxidized in air at various oxide thicknesses, $h = 0$, 1, 2 and 3 μm, at 1200 °C for batches I, II and III are shown in Fig. 10(a), (b) and (c), respectively. As the TGO thickness increases, the total load for a given strain increases; this means that the TGO formed on the surface substantially reinforced the specimens. The TGO scales formed on all three batches were observed to be of nearly uniform thickness across the entire interface and composed entirely of α-phase alumina. Therefore, assuming no interaction between the substrate and TGO, the TGO stress, σ_{TGO}, for a tensile specimen is been calculated by using the following equation:

$$\sigma_{TGO} \approx \frac{P - \sigma_M HW}{2hW},$$

where H is the thickness of the substrate, h is the TGO thickness, σ_M is the stress imposed on the substrate, P is the total load and W is the specimen width, as illustrated in Fig. 6. This equation means that the load imposed on the TGO is calculated by subtracting the load due to the stress imposed on the substrate metal itself from the total load. Fig. 11(a), (b) and (c) shows the σ_{TGO}–ε curves for specimens of batches I, II, and III, respectively. In each figure, three σ_{TGO}–ε curves are plotted for three different TGO thicknesses, h. Even though there are significant scatters, all the curves have a consistent feature, regardless of the batches, that is, regardless of the yttrium contents. Namely, after the initial yield point, the stress rapidly drops to a certain limit and then increases again gradually. Fig. 11(a) shows that the TGO formed on batch-I specimen has the yield stress of 75–85 MPa

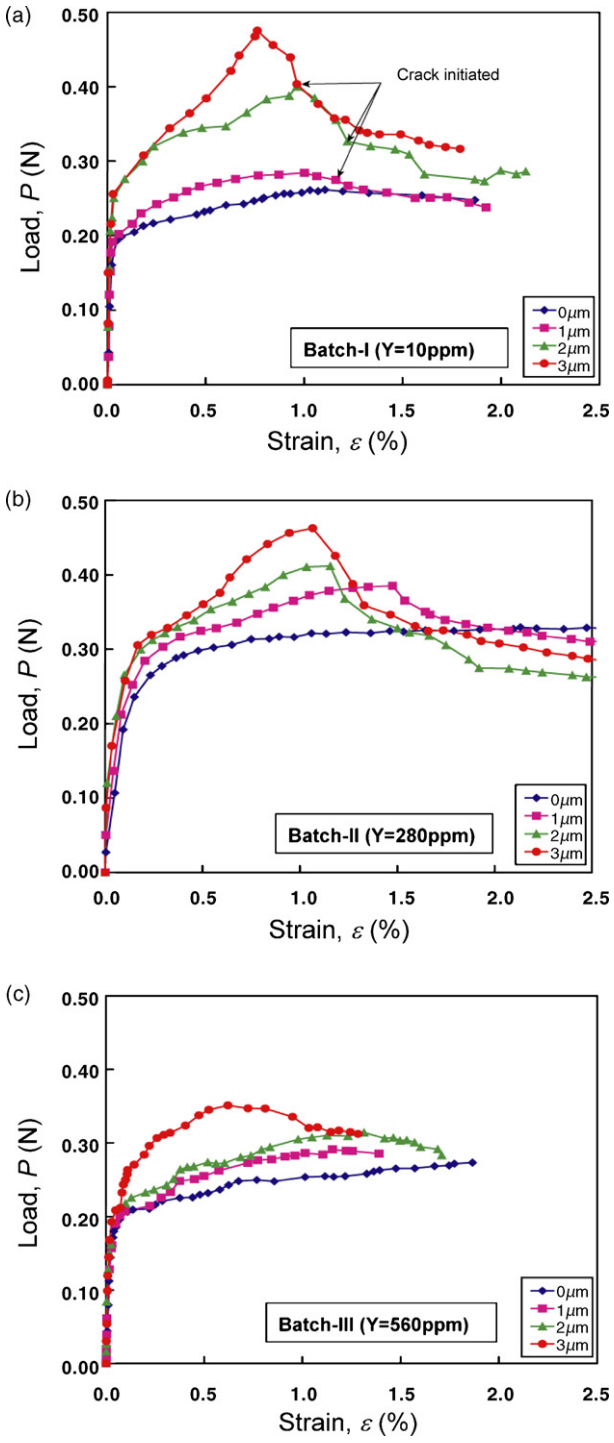

Fig. 10. Load–strain curves measured from tension tests of specimens oxidized in air at 1200 °C with TGO thickness variation (0, 1, 2 and 3 μm) (a) batch-I (Y: 10 ppm), (b) batch-II (Y: 280 ppm) and (c) batch-III (Y: 560 ppm).

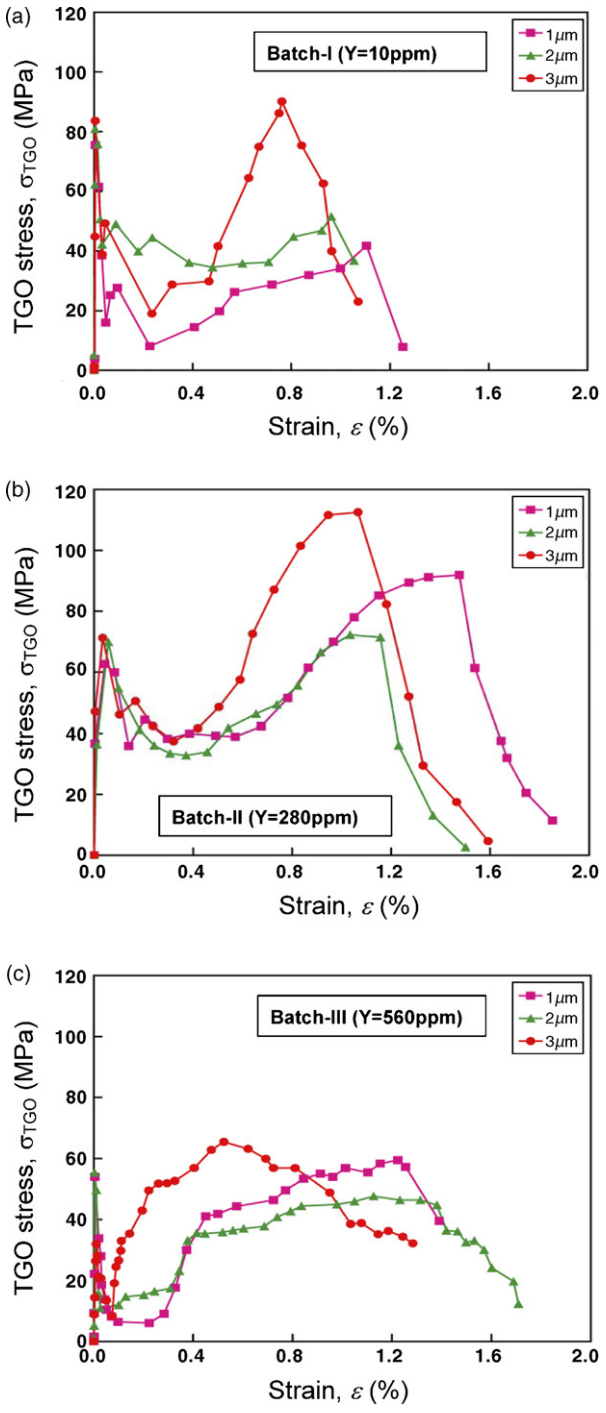

Fig. 11. Stress–strain curves of TGO formed at 1200 °C (a) batch-I (Y: 10 ppm), (b) batch-II (Y: 280 ppm) and (c) batch-III (Y: 560 ppm).

Table 3
Tensile properties of Al_2O_3 TGO formed on Fecralloy foils at 1200 °C

Batch	Y content (ppm)	Yield stress, σ_Y (MPa)	Ultimate tensile strength, σ_{UTS} (MPa)	ε at σ_{UTS} (%)
I	10	75–85	60–80	0.8–1.0
II	280	65–70	80–110	1.0–1.5
III	560	40–60	50–60	0.6–1.2

and ultimate tensile strength of 60–80 MPa. Fig. 11(b) and (c), however, show that the TGOs formed on batches II and III have the yield stress of 65–70 and 40–60 MPa and ultimate tensile strength of 80–110 and 50–60 MPa, respectively. The strain at the ultimate tensile strength ranges 0.6–1.5%. On the whole, the TGO formed on batch-II is strongest. These tensile properties are summarized in Table 3.

To the authors' knowledge, no data on the tensile properties of thermally grown alumina formed on a metal substrate at such a high temperature has been reported in literatures. Even for bulk polycrystalline alumina, the tensile properties at high temperatures are hardly found. According to a review paper by Munro, the ultimate tensile strength of bulk alumina with grain sizes of 1–6 μm is about 130 MPa at 1200 °C.[40] No detailed stress–strain curves are available. Compared with 130 MPa, the tensile strength of α-Al_2O_3 TGO formed on Fecralloy at the same temperature was found to be somewhat lower but comparable. And the unique feature of the stress–strain curves of TGO and the substantial deformation before final break are unexpected. As shown in Fig. 10(a) to (c), the α-Al_2O_3 TGO provides good mechanical protection, tolerating deformation up to 1–2% strain, as well as good protection against high temperature corrosion. This might be the reason why the α-Al_2O_3 TGO is preferred in applications subjected to thermal cycling such as gas turbine components.

Despite of the large scatter, the effect of Y content on the tensile properties of TGO itself is significant, as shown in Figs. 10 and 11. The reason for this is yet to be solved. The chemical composition was analyzed with EDS and back scattering electron imaging,[36] but meaningful results could not be obtained due to the limited precision of the techniques. The answer may be provided by a study of the microstructural difference among the TGOs, which will be investigated in a future work.

4. Conclusion

New material test systems based on Joule heating and a new TGO thickness sensor, which enables *in situ* monitoring on a specimen surface at high temperature, have been used to measure the creep and tensile properties of thermally grown oxide (TGO) alumina formed on metal foils at 1200 °C. Three batches of Fecralloy foils, which differ from each other in contents of yttrium, that is, 10, 280 and 560 ppm, respectively, were chosen as the TGO forming substrate. The following conclusions were obtained from the results:

(i) Creep rates of TGO α-Al_2O_3 films on Fecralloy substrates were much higher than those observed in bulk polycrystalline alumina. Creep rates decreased as the TGO thickness increased. These two findings agree with the hypothesis that the high temperature creep of TGO is a consequence of inter-grain growth of the TGO.

(ii) Y-content of 560 ppm in the Fecralloy substrate delayed the creep rate of the TGO formed on it, while the Y-content of 280 ppm did not produce any significant difference in the creep properties from those of the TGO formed on the substrate with Y-content of 10 ppm (virtually zero).

(iii) Even though there were significant scatters, the tensile stress–strain curves of the TGO formed on the three batches showed a common feature. Namely, after the initial yield point, the stress rapidly dropped to a certain limit and then increased again gradually. Consequently, the α-Al_2O_3 TGO provided good mechanical protection tolerating deformation up to 1–2% strain as well as good protection against high temperature corrosion.

(iv) The yield stress of the TGO ranged from 40 to 85 MPa and ultimate tensile strength ranged from 50 to 110 MPa. On the whole, the TGO formed on batch-II was strongest and toughest. These strengths were somewhat lower or comparable to previous data of stand-alone polycrystalline alumina.

Acknowledgments

This work was performed under the program of Basic Atomic Energy Research Institute (BAERI), which is a part of the Nuclear R&D Programs of the Ministry of Science & Technology (MOST), and one of the authors, S.K. Sharma, financially supported by BK-21 program, Republic of Korea. Appreciation is extended to Prof. A.G. Evans for initial inspiration and valuable discussions.

References

1. Birks, N., Meier, G. H. and Pettit, F. S., *Introduction to the High Temperature Oxidation of Metals*. Cambridge University Press, Cambridge, 2006.
2. Pieraggi, B., Comments on growth of alumina scales on Fe–Cr–Al alloys. *Oxid. Met.*, 2005, **64**, 397–403.
3. Nychka, J. A. and Clarke, D. R., Quantification of aluminum outward diffusion during oxidation of FeCrAl alloys. *Oxid. Met.*, 2005, **63**, 325–352.
4. Quadakkers, W. J., Naumenko, D., Wessel, E., Kochubey, V. and Singheiser, L., Growth rate of alumina scales on Fe–Cr–Al alloys. *Oxid. Met.*, 2004, **61**, 17–37.
5. Tolpygo, V. K. and Clarke, D. R., In *Proceedings of the 5th International Conference on Microscopy of Oxygen*, 2002, pp. 1–23.
6. Evans, A. G., Mumm, D. R., Hutchinson, J. W., Meier, G. H. and Pettit, F. S., Mechanism of controlling the durability of thermal barrier coatings. *Prog. Mater. Sci.*, 2001, **46**, 505–553.
7. Grabke, H. J., Surface and interface segregation in the oxidation of metals. *Surf. Interf. Anal.*, 2000, **30**, 112–119.
8. Sidique, S. E., Mollah, A. H., Islam, M. S., Ali, M. M., Megat, M. H. H. and Basri, S., High temperature oxidation behavior of iron–chromium–aluminum alloys. *Oxid. Met.*, 2000, **54**, 385–400.
9. Schutze, M., *Protective Oxide Scale and their Breakdown*. John Wiley and Sons, England, 1997.
10. Tolpygo, V. K. and Clarke, D. R., Alumina scale failure resulting from stress relaxation. *Surf. Coat. Technol.*, 1999, **120–121**, 1–7.
11. Schwarzer, J., Lohe, D. and Vohringer, O., Influence of the TGO creep behavior on delamination stress development in thermal barrier coating systems. *Mater. Sci. Eng. A*, 2004, **387**, 692–695.
12. Karadge, M., Zhao, X., Preuss, M. and Xiao, P., Microstructure of the thermally grown alumina in commercial thermal barrier coatings. *Scripta Mater.*, 2006, **54**, 639–644.
13. Kang, K. J., Hutchinson, J. W. and Evans, A. G., Measurement of the strains induced upon thermal oxidation of an alumina-forming alloy. *Acta Mater.*, 2003, **51**, 1283–1291.
14. Ray, A. K. and Das, D. K., Accelerated creep resistance of thermal barrier coated superalloy. *Mater. Lett.*, 2006, **60**, 3019–3022.

15. Mennicke, C., Schumann, E., Ruhle, M., Hussey, R. J., Sproule, G. L. and Graham, M. J., The effect of yttrium on the growth process and microstructure of α-Al_2O_3 on FeCrAl. *Oxid. Met.*, 1998, **49**, 455–466.
16. Liu, Z., Gao, W. and He, Y., Modeling of oxidation kinetics of Y-doped Fe–Cr–Al alloys. *Oxid. Met.*, 2000, **53**, 341–350.
17. Cueff, R., Buscail, H., Caudron, E., Issartel, C. and Riffard, F., Influence of yttrium alloying addition on the oxidation of alumina formers at 1173 K. *Oxid. Met.*, 2002, **58**, 439–455.
18. Cueff, R., Buscail, H., Caudron, E., Riffard, F., Issartel, C. and Messki, S. E., Effect of reactive element oxide coating on the high temperature oxidation behavior of FeCrAl alloys. *Appl. Surf. Sci.*, 2004, **229**, 233–241.
19. Hamid, A. U., TEM study of the effect of Y on the scale microstructures of Cr_2O_3 and Al_2O_3 forming alloys. *Oxid. Met.*, 2002, **58**, 23–40.
20. Wang, L. and Li, D. Y., Effect of yttrium on microstructure, mechanical properties and high-temperature wear behavior of cast satellite 6 alloy. *Wear*, 2003, **255**, 535–544.
21. Tolpygo, V. K., The morphology of thermally grown α-Al_2O_3 scales on Fe–Cr–Al alloys. *Oxid. Met.*, 1999, **51**, 449–477.
22. Mumm, D. R. and Evans, A. G., On the role of imperfections in the failure of a thermal barrier coating made by electron beam deposition. *Acta Mater.*, 2000, **48**, 1815–1827.
23. Amano, T., Isobe, H., Sakai, N. and Shishido, T., The effects of yttrium addition on high temperature oxidation of heat resistant alloy with sulfur. *J. Alloys Compd.*, 2002, **344**, 394–400.
24. Kadiri, H. E., Bienvenu, Y., Solanki, K., Horstemeyer, M. F. and Wang, P. T., Creep and tensile behavior of Fe–Cr–Al foils and laser micro-welds at high temperature. *Mater. Sci. Eng. A*, 2006, **421**, 168–181.
25. Pastor, J. Y., Lorca, J. L., Salazar, A., Oliete, P. B., Francisco, I. D. and Pena, J. I., Mechanical properties of melt-grown alumina-yttrium aluminum. *J. Am. Ceram. Soc.*, 2005, **88**, 1488–1495.
26. Spigarelli, S., Cabibbo, M., Evangelista, E. and Cucchieri, S., Evaluation of the creep properties of an Al–17Si–Mg–0.7Cu alloy. *Mater. Lett.*, 2002, **56**, 1059–1063.
27. Yue, X. M., Zhang, G. J., Watanabe, T. and Tai, W. P., Corrosion behavior of single crystal alumina in argon, air, and water vapor atmospheres at 1700–2000 °C. *J. Am. Ceram. Soc.*, 1999, **82**, 2560–2562.
28. Cho, J. H., Harmer, M. P., Chan, H. M., Rickman, J. M. and Thompson, A. M., Effect of yttrium and lanthanum on the tensile creep behavior of aluminum oxide. *J. Am. Ceram. Soc.*, 1997, **80**, 1013–1017.
29. Fang, J., Thompson, A. M., Harmer, M. P. and Chan, H. M., Effect of yttrium and lanthanum on the final-stage sintering behavior of ultrahigh purity alumina. *J. Am. Ceram. Soc.*, 1997, **80**, 2005–2012.
30. French, J. D., Zhao, J., Harmer, M. P., Chan, H. M. and Miller, G. A., Creep of duplex microstructures. *J. Am. Ceram. Soc.*, 1994, **77**, 2857–2865.
31. Cannon, R. M., Rhodes, W. H. and Heuer, A. H., Plastic deformation of fine-grained alumina (Al_2O_3): I, interface-controlled diffusional creep. *J. Am. Ceram. Soc.*, 1980, **63**, 46–53.
32. Cobble, R. L., A model for boundary diffusion controlled creep in polycrystalline materials. *J. Appl. Phys.*, 1963, **34**, 1679–1682.
33. Echsler, H., Ito, S. and Schutze, M., Mechanical properties of oxide scales on mild steel at 800–1000 °C. *Oxid. Met.*, 2003, **60**, 241–269.
34. Bruns, C. and Schutze, M., Investigation of the mechanical properties of oxide scales on nickel and TiAl. *Oxid. Met.*, 2001, **155**, 35–68.
35. Schutze, M., Ito, S., Przybilla, W., Echsler, H. and Bruns, C., Test methods and data on the mechanical properties of protective oxide scales. *Mater. High Temp.*, 2001, **18**, 39–50.
36. Kang, K. J. and Mercer, C., Creep properties of thermally grown alumina. *Mater. Sci. Eng. A*, 2008, **478**, 154–162.
37. Lee, S. S., Sun, S. K. and Kang, K. J., In-situ measurement of the thickness of aluminum oxide scales at high temperature. *Oxid. Met.*, 2005, **63**, 73–85.
38. Lang, E., *The Role of Active Elements in the Oxidation Behavior of High Temperature Metals and Alloys*. Elsevier, London, 1989.
39. Dassios, K. G., Steen, M. and Filiou, C., Mechanical properties of alumina Nextel^{TM} 720 fibers at room and elevated temperatures: tensile bundle testing. *Mater. Sci. Eng. A*, 2003, **349**, 63–72.
40. Munro, R. G., Evaluated material properties for a sintered α-alumina. *J. Am. Ceram. Soc.*, 1997, **80**, 1919–1928.